ARTICLE

BIOTECHNOLOGY and BIOENGINEERING

Improving Product Yields on D-Glucose in *Escherichia coli* Via Knockout of *pgi* and *zwf* and Feeding of Supplemental Carbon Sources

Eric Shiue, Irene M. Brockman, Kristala L. J. Prather

Department of Chemical Engineering, Synthetic Biology Engineering Research Center (SynBERC), Massachusetts Institute of Technology, Cambridge, Massachusetts 02139; telephone: 617-253-1950; fax: 617-258-5042; e-mail: kljp@mit.edu

ABSTRACT: The use of lignocellulosic biomass as a feedstock for microbial fermentation processes presents an opportunity for increasing the yield of bioproducts derived directly from glucose. Lignocellulosic biomass consists of several fermentable sugars, including glucose, xylose, and arabinose. In this study, we investigate the ability of an *E. coli* Δ*pgi* Δ*zwf* mutant to consume alternative carbon sources (xylose, arabinose, and glycerol) for growth while reserving glucose for product formation. Deletion of *pgi* and *zwf* was found to eliminate catabolite repression as well as the ability of *E. coli* to consume glucose for biomass formation. In addition, the yield from glucose of the bioproduct D-glucaric acid was significantly increased in a Δ*pgi* Δ*zwf* strain.

Biotechnol. Bioeng. 2015;112: 579–587.

KEYWORDS: product yield; strain engineering; biomass; D-glucaric acid

Introduction

In recent years, concerns over declining petroleum reserves and climate change due to atmospheric carbon dioxide accumulation have spurred significant interest in using alternative feedstocks for the manufacture of petroleum-derived products. Because it is renewable and abundant, non-food plant (lignocellulosic) biomass represents a promising alternative feedstock to crude oil. Moreover, because plants assimilate carbon dioxide during growth, the use of plant-based feedstocks could potentially slow the accumulation of carbon dioxide in the atmosphere. Recent research has focused heavily on the identification of ideal plant biomass feedstocks (Joyce and Stewart, 2012), the determination of commercially valuable, biomass-derived products (Werpy and Petersen, 2004), and the development of processes for converting plant biomass into these products of interest.

One such process that has received heavy attention is microbial fermentation. A significant portion of lignocellulosic biomass consists of fermentable sugars such as glucose, xylose, arabinose, and galactose (Joyce and Stewart, 2012), and many microbes are naturally able to convert these sugars into products of interest such as biochemicals and biopolymers (Lee, 1996). In addition, microbes can be engineered to produce a wide array of non-natural products via recombinant DNA technology (Curran and Alper, 2012). A few products, including D-glucaric acid (Moon et al., 2009) and D-gluconic acid (Rogers et al., 2006), are derived directly from glucose; however, microbial production of these products generally suffers from low yields, as a portion of the glucose feed is utilized to generate cell biomass. For products such as these that do not require further glucose metabolism through the canonical reduction pathways, eliminating the ability to utilize glucose for growth may address this limitation. We thus set out to design an *E. coli* production platform that utilizes an alternative carbon source such as arabinose or xylose for cell growth, reserving glucose solely for product generation to maximize yield.

The main pathways for glucose utilization in *E. coli* are depicted in Figure 1. Glucose enters the cell through the phosphotransferase system (PTS) encoded by *ptsG* and *ptsHIcrr* and is phosphorylated to glucose-6-phosphate in the process. Glucose-6-phosphate can then proceed through the Entner–Dudoroff Pathway via *zwf* or through the Embden–Meyerhoff–Parnas Pathway via *pgi*. The carbon in glucose-6-phosphate can also be stored as glycogen via *pgm*. Previous work to engineer *E. coli* for co-utilization of glucose and alternative carbon sources involved deleting the PTS system

Correspondence to: K.L.J. Prather

Contract grant sponsor: National Science Foundation through the Synthetic Biology Engineering Research Center
Contract grant number: EEC-0540879
Contract grant sponsor: CAREER Award Program
Contract grant number: CBET-0954986
Contract grant sponsor: Biotechnology Training Program of the National Institutes of Health
Contract grant number: T32GM008334
Received 2 July 2014; Revision received 5 September 2014; Accepted 19 September 2014
Accepted manuscript online 25 September 2014;
Article first published online 24 November 2014 in Wiley Online Library (http://onlinelibrary.wiley.com/doi/10.1002/bit.25470/abstract).
DOI 10.1002/bit.25470

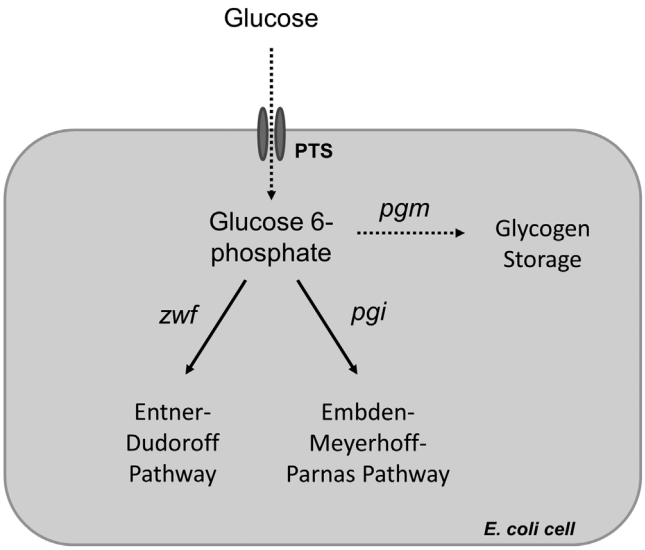

Figure 1. Glucose utilization pathways in *E. coli*.

(Balderas-Hernández et al., 2011; Solomon et al., 2013; Wang et al., 2011). By eliminating the PTS system, catabolite repression can be eliminated, allowing simultaneous uptake of glucose and a secondary carbon source. However, these strategies also eliminate *E. coli*'s primary method of glucose uptake, and the cell must rely on non-specific transporters to import glucose into the cell. Subsequent phosphorylation of glucose to glucose-6-phosphate via ATP-dependent *glk* is also required for glucose metabolism in PTS-deficient *E. coli*. Overexpression of the galactose:H^+ symporter *galP* and upregulation of *glk* has been shown to recover wild-type growth rates in PTS-deficient strains of *E. coli* (Hernández-Montalvo et al., 2003). However, because glycolytic pathways remain intact in this strain, it is likely that product yields on glucose would remain low. In this study, we explore the behavior of an *E. coli* strain that lacks *pgi* and *zwf* and investigate this strain's ability to produce a glucose-derived product when supplemented with L-arabinose and D-xylose, sugars which are readily available from biomass. Glycerol is also explored as a carbon source, as its price has dropped significantly in recent years due to significant increases in biodiesel production (Johnson and Taconi, 2009). Previous work has demonstrated improved yield of glucose-derived products in a Δ*pgi* Δ*zwf* strain supplemented with mannitol (Kogure et al., 2007; Pandey et al., 2013); however, the price of mannitol remains high relative to glycerol and biomass-derived sugars.

Materials and Methods

E. coli Strains and Plasmids

E. coli strains, plasmids, and oligonucleotides used in this study are listed in Table I. All molecular biology manipulations were performed according to standard practices (Sambrook and Russell, 2001). *E. coli* DH10B was used for transformation of cloning reactions and propagation of all plasmids. Strains M2, M2-2, and M3 were constructed by our group previously (Gonçalves et al., 2013; Shiue and Prather, 2014). Strain M2 was generated via knockout of *endA* and *recA* from *E. coli* MG1655. Strain M2-2 was generated via knockout of *gudD* and *uxaC* from strain M2 to prevent consumption of D-glucaric and D-glucuronic acids during D-glucaric acid production experiments. Strain M3 was derived from strain M2 via knockout of *pgi* and served as an intermediate strain; this strain was not further characterized in this work. Deletion of *zwf* from strain M3 was achieved by P1 transduction with Keio collection strain JW1841-1 as the donor (Baba et al., 2006). The λDE3 lysogen was then integrated site-specifically into this quadruple knockout strain using a λDE3 Lysogenization Kit (Novagen, Darmstadt, Germany), generating strain M4 (MG1655(DE3) Δ*endA* Δ*recA* Δ*pgi* Δ*zwf*. To prevent *E. coli* from consuming D-glucuronic and D-glucaric acids, both *gudD* and *uxaC* were deleted from the genome. Deletion of *uxaC* was performed with λ-Red mediated recombination (Datsenko and Wanner, 2000) using pKD46recA (Solomon et al., 2013). PCR primers pKD13_uxaC_fwd and pKD13_uxaC_rev (Table I) were used to amplify the recombination cassette from pKD13 (Datsenko and Wanner, 2000), and strain M4 harboring pKD46recA was transformed with this PCR product. The *kan* selection cassette was cured from successful deletion mutants using FLP recombinase expressed from pCP20, generating strain M5. Similar to strain M3, strain M5 served as an intermediate strain only and was not further characterized in this work. Finally, strain M6 (MG1655(DE3) Δ*endA* Δ*recA* Δ*pgi* Δ*zwf* Δ*uxaC* Δ*gudD*) was generated using the same λ-Red mediated recombination method described above; in this case, primers pKD13_gudD_fwd and pKD13_gudD_rev were used to amplify the recombination cassette from pKD13. pRSFD-IN and pTrc-Udh were constructed by our group previously (Moon et al., 2009; Yoon et al., 2009). To construct pRSFD-IN-Udh, pRSFD-IN was first digested with *Xho*I, end-filled with Klenow enzyme, then digested with *Eco*RI-compatible *Mfe*I. pTrc-Udh was then digested with *Eco*RI and *Sma*I, and the Udh-containing fragment was ligated into digested pRSFD-IN to generate pRSFD-IN-Udh.

Culture Conditions

For determination of growth curves, cultures were grown in 250 mL baffled shake flasks containing 50 mL LB medium supplemented with approximately 10 g/L D-glucose, L-arabinose, glycerol, and/or D-xylose as indicated in Figures 2–5. Seed cultures were grown overnight at 30°C and inoculated to an optical density at 600 nm (OD_{600}) of 0.005. Cultures were incubated at 30°C, 250 rpm, and 80% relative humidity for 72 h. To construct a growth curve, cell densities were measured at regular time intervals on a DU800 Spectrophotometer (Beckman Coulter, Pasadena, CA), with more frequent sampling during the exponential growth phase. For analysis of metabolite concentrations, samples were taken daily,

Table I. *E. coli* strains, plasmids, and oligonucleotides used.

Name	Relevant genotype	Reference
Strains		
DH10B	F⁻ *mcrA* Δ*(mrr-hsdRMS-mcrBC) φ80lacZ*Δ*M15* Δ*lacX74 recA1 endA1 araD139*Δ*(ara, leu)7697 galU galK* λ*-rpsL nupG*	Life Technologies (Carlsbad, CA)
JW1841-1	F⁻, Δ*(araD-araB)567,* Δ*lacZ4787(::rrnB-3),* λ⁻, Δ*zwf-777::kan, rph-1,*Δ*(rhaD-rhaB)568, hsdR514*	CGSC #9537 (Baba et al., 2006)
MG1655	F⁻ λ⁻ *ilvG⁻ frb-50 rph-1*	ATCC #700926
M2	MG1655(DE3) Δ*endA* Δ*recA*	Shiue and Prather (2014)
M2-2	MG1655(DE3) Δ*endA* Δ*recA* Δ*gudD* Δ*uxaC*	Shiue and Prather (2014)
M3	MG1655 Δ*endA* Δ*recA* Δ*pgi*	Gonçalves et al. (2013)
M4	MG1655(DE3) Δ*endA* Δ*recA* Δ*pgi* Δ*zwf*	This study
M5	MG1655(DE3) Δ*endA* Δ*recA* Δ*pgi* Δ*zwf* Δ*uxaC*	This study
M6	MG1655(DE3) Δ*endA* Δ*recA* Δ*pgi* Δ*zwf* Δ*uxaC* Δ*gudD*	This study
Plasmids		
pCP20	Rep[a], Amp^R, Cm^R, FLP recombinase expressed by λ p_r under control of λ cI857	CGSC #7629
pKD13	R6Kγ *ori*, Amp^R, *kan*	CGSC #7633
pKD46	R101 *ori*, *repA101*[a], Amp^R, *araC*, *araBp*-λ_γ-λ_β-λ_{exo}	CGSC #7739
pKD46recA	R101 *ori*, *repA101*[a], Amp^R, *araC*, *araBp*-λ_γ-λ_β-λ_{exo}, *recA*	Solomon et al. (2013)
pRSFDuet-1	pRSR1030 *ori*, lacI, Kan^R	EMD4 Biosciences (Darmstadt, Germany)
pTrc99A	pBR322 *ori*, Amp^R	Amann and Brosius (1985)
pRSFD-IN	pRSFDuet-1 with INO1 inserted into the *Eco*RI and *Hin*dIII sites	Moon et al. (2009)
pTrc-Udh	pTrc99A with Udh from *Pseudomonas syringae* inserted into the *Nco*I and *Hin*dIII sites	Moon et al. (2009), Yoon et al. (2009)
pRSFD-IN-Udh	pRSFD-IN with Udh inserted into the *Mfe*I and *Xho*I sites	This study
pTrc-SUMO-MIOX	pTrc99A with SUMO-MIOX	Shiue and Prather (2014)
Oligonucleotides	5′ → 3′ Sequence[a]	
pKD13_gudD_fwd	TCCCCGGCTGGACCTTTGACCGTAAACGTCCCGTTTTCGGCCGTCATTGATTCTGAAAAAGGACATAAATCTGTCAAACATGAGAATTAATTCC	
pKD13_gudD_rev	CAACAGGCTATTTTGCGTTTAGCATCAGTCTCAAACCGGCTCCAGATAGAGCCGGTTTTGGTTTTCTGTCGTGTAGGCTGGAGCTGCTTC	
pKD13_uxaC_fwd	AATTGGTGTGATAACTTTGTCAGCATCGCACCATAAGCAAGCTAGCTCACTCGTTGAGAGGAAGACGAAACTGTCAAACATGAGAATTAATTCC	
pKD13_uxaC_rev	AAATCTGCTAAAGCGACCGCGACGTTATCCAGCGCATGGATCTTGATGTATTGCATATCAACCCCAGACCGTGTAGGCTGGAGCTGCTTC	

[a]All oligonucleotides purchased from Sigma–Genosys (St. Louis, MO). Homologous sequences used for recombination are underlined.

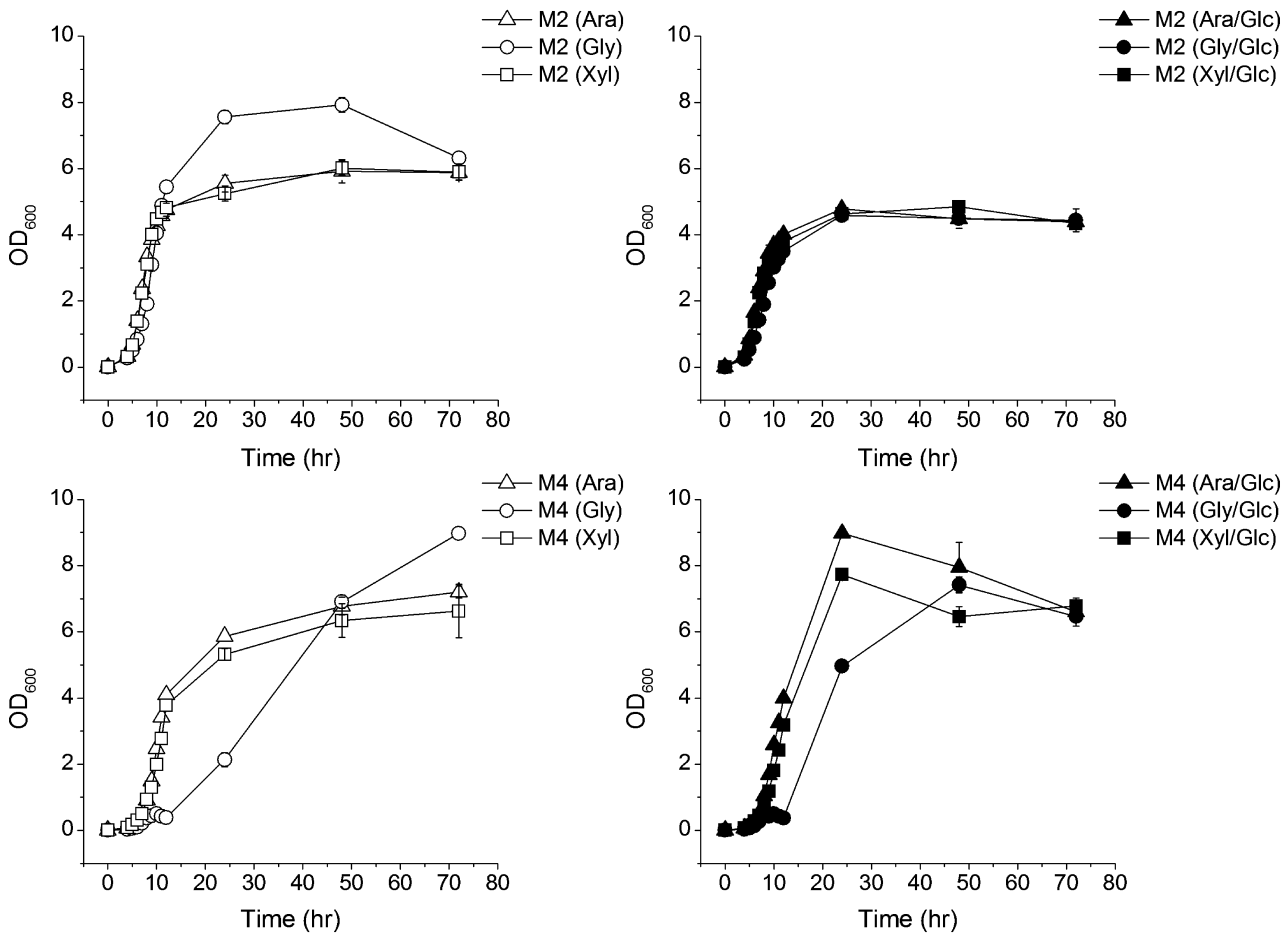

Figure 2. Growth curves for strains M2 (**top row**) and M4 (**bottom row**) in rich medium supplemented with L-arabinose ("Ara," triangles), glycerol ("Gly," circles), and D-xylose ("Xyl," squares) with D-glucose ("Glc") absent (open points) or present (filled points). M2: MG1655(DE3) Δ*endA recA*; M4: MG1655(DE3) Δ*endA* Δ*recA* Δ*pgi* Δ*zwf*.

centrifuged to remove cell debris, and the supernatants analyzed via high-performance liquid chromatography (HPLC) as described in the Determination of Metabolite Concentrations section.

For glucaric acid production in rich medium, cultures were grown in 250 mL baffled shake flasks containing 50 mL LB medium supplemented with 10 g/L D-glucose and 10 g/L L-arabinose, 10 g/L glycerol, or 10 g/L D-xylose. Cultures were induced at inoculation with 0.1 mM isopropyl-β-D1-thiogalactopyranoside (IPTG). Ampicillin (100 μg/mL) and kanamycin (30 μg/mL) were added for plasmid maintenance. Seed cultures were grown overnight at 30°C in LB medium supplemented with 10 g/L D-glucose and 10 g/L L-arabinose, 10 g/L glycerol, or 10 g/L D-xylose and inoculated to an OD_{600} of 0.005. Cultures were incubated at 30°C, 250 rpm, and 80% relative humidity for 72 h. Adequate aeration for product formation was ensured with the use of baffled shake flasks. Samples were taken daily, centrifuged to remove cell debris, and the supernatants analyzed for metabolite concentrations.

For minimal medium experiments, a modified MOPS-buffered medium was used containing 10 g/L D-glucose, 6 g/L L-arabinose, 6 g/L NH_4Cl, 0.4 g/L K_2HPO_4, 2 mM $MgSO_4$, 0.1 mM $CaCl_2$, 40 mM MOPS, 4 mM tricine, 50 mM NaCl, 100 mM Bis-Tris, 134 μM EDTA, 31 μM $FeCl_3$, 6.2 μM $ZnCl_3$, 0.76 μM $CuCl_2$, 0.42 μM $CoCl_2$, 1.62 μM H_3BO_3, 0.081 μM $MnCl_2$, carbenicillin (100 μg/mL), and kanamycin (30 μg/mL). Seed cultures were started using a 1:100 dilution from LB and were grown at 30°C for 48 h in modified MOPS. Working cultures were inoculated to an OD_{600} of 0.02 and induced 32 h after inoculation with 0.1 mM IPTG. Cultures were incubated at 30°C, 250 rpm, and 80% relative humidity for 110 h. Adequate aeration for product formation was ensured with the use of baffled shake flasks. Samples were taken periodically, centrifuged to remove cell debris, and the supernatants analyzed for metabolite concentrations.

Determination of Metabolite Concentrations

D-glucose, L-arabinose, glycerol, D-xylose, and D-glucaric acid were quantified from culture supernatants using HPLC on an

Agilent Series 1100 or Series 1200 instrument equipped with an Aminex HPX-87H column (300 mm × 7.8 mm; Bio-Rad Laboratories, Hercules, CA). Sulfuric acid (5 mM) was used as the mobile phase at 35°C and a flow rate of 0.6 mL/min in isocratic mode. Compounds were detected and quantified from 10 μL sample injections using refractive index and diode array detectors. Reported metabolite concentrations are the average of triplicate samples, and error bars represent one standard deviation above and below the mean value.

Results

In *E. coli*, glucose is imported into the cell and phosphorylated to glucose 6-phosphate (G6P) by the PTS. Glucose metabolism then proceeds through two routes (Fig. 1): the Embden–Meyerhoff–Parnas Pathway via phosphoglucose isomerase (*pgi*) or the Entner–Dudoroff Pathway via glucose 6-phosphate dehydrogenase (*zwf*). A third route interconverts glucose 6-phosphate and glucose 1-phosphate via phosphoglucomutase (*pgm*) for glycogen storage and accumulation, though flux through this node is typically extremely low (Chassagnole et al., 2002). To eliminate native consumption of glucose, both *pgi* and *zwf* were deleted from an MG1655-derived strain. Growth on M9 minimal medium supplemented with various carbon sources confirmed that the Δ*pgi* Δ*zwf* mutant does not grow on glucose but retains the ability to utilize other carbon sources (Supplementary Figs. S1 and S2).

Behavior of a Δ*pgi* Δ*zwf* Mutant

Cell growth was compared for strains M2 and M4, a Δ*pgi* Δ*zwf* mutant in rich medium supplemented with various carbon sources (Fig. 2). Maximum specific growth rates for each combination of strain and carbon supplement were also calculated (Table II). As expected, growth of strain M2 was similar for all conditions tested, with similar lag phases and maximum specific growth rates. Final cell densities were lower when strain M2 was fed D-glucose, likely due to increased production of acetate (Fig. 3), which has been shown to inhibit cell growth (Roe et al., 1998). Growth of strain M4 was also similar for all conditions tested with the exception of glycerol-supplemented cultures, which displayed a significant lag in growth of approximately 24 h. We hypothesize that this lag corresponds to depletion of the metabolic precursors provided by LB and a metabolic shift toward gluconeogenic metabolism for growth on glycerol. Maximum growth rate, lag time, and final cell densities are similar for strain M4 in the presence of L-arabinose, glycerol, and D-xylose regardless of whether D-glucose was supplemented in the growth medium, indicating that substrate consumption was similar in the presence or absence of D-glucose. Overall, maximum growth rates of strain M4 were approximately 70% that of strain M2.

Table II. Maximum growth rates of various strains in rich medium supplemented with various carbon sources.

Strain[a]	Alternative carbon source	Glucose	μ_{max} (h^{-1})
M2	L-Arabinose	−	1.00 ± 0.01
		+	1.01 ± 0.06
	Glycerol	−	0.98 ± 0.02
		+	0.97 ± 0.04
	D-Xylose	−	1.00 ± 0.03
		+	0.87 ± 0.20
M4	L-Arabinose	−	0.65 ± 0.01
		+	0.66 ± 0.02
	Glycerol	−	0.66 ± 0.05
		+	0.68 ± 0.01
	D-Xylose	−	0.70 ± 0.01
		+	0.67 ± 0.01

[a]M2: MG1655(DE3) Δ*endA* Δ*recA*; M4: MG1655(DE3) Δ*endA* Δ*recA* Δ*pgi* Δ*zwf*.

Concentrations of D-glucose, alternative carbon source, and acetate were measured for each strain/carbon supplement combination as a function of time (Fig. 3). As expected, the presence of D-glucose prevents consumption of the alternative carbon source in strain M2 via catabolite repression. In contrast, the deletion of *pgi* and *zwf* prevents consumption of D-glucose in strain M4. Interestingly, deletion of *pgi* and *zwf* appears to eliminate catabolite repression in strain M4, as the presence of D-glucose does not preclude consumption of the alternative carbon source in this strain.

This elimination of catabolite repression is perhaps due to intracellular buildup of glucose-6-phosphate. Catabolite repression is mediated by cyclic AMP (cAMP), which is synthesized by adenylate cylcase. Adenylate cylcase is activated via phosphorylation by $EIIA^{Glc}$, but this phosphorylation can only occur if $EIIA^{Glc}$ has a phosphate group to donate. When glucose is being actively imported through the PTS system, $EIIA^{Glc}$ donates its phosphate to the incoming glucose, resulting in a mostly unphosphorylated population of $EIIA^{Glc}$, inactive adenylate cyclase, and a low concentration of cAMP. The absence or depletion of glucose from the culture medium leads to a buildup of phosphorylated $EIIA^{Glc}$, activation of adenylate cyclase, and an increase in cAMP concentration, eventually leading to the expression of catabolite-repressed genes such as *araBAD* and *xylAB*, which are important for arabinose and xylose metabolism, respectively. Thus, catabolite repression occurs when there is active glucose flux into the cell, not simply when glucose is present in the medium. In a Δ*pgi* Δ*zwf* mutant, the accumulation of glucose-6-phosphate quickly eliminates glucose flux into the cell, resulting in the derepression of genes normally repressed in the presence of glucose.

D-Glucaric Acid Production in a Δ*pgi* Δ*zwf* Mutant

D-Glucaric acid, a dicarboxylic organic acid, is a naturally occurring product, that has been investigated for a variety of potential applications. A biosynthetic pathway to D-glucaric acid from D-glucose has been constructed in *E. coli* (Moon et al., 2009). This pathway begins with glucose-6-phosphate, which is converted to *myo*-inositol-1-phosphate by *myo*-inositol-1-phosphate synthase (INO1). *Myo*-inositol-1-phosphate is then dephosphorylated by an endogenous

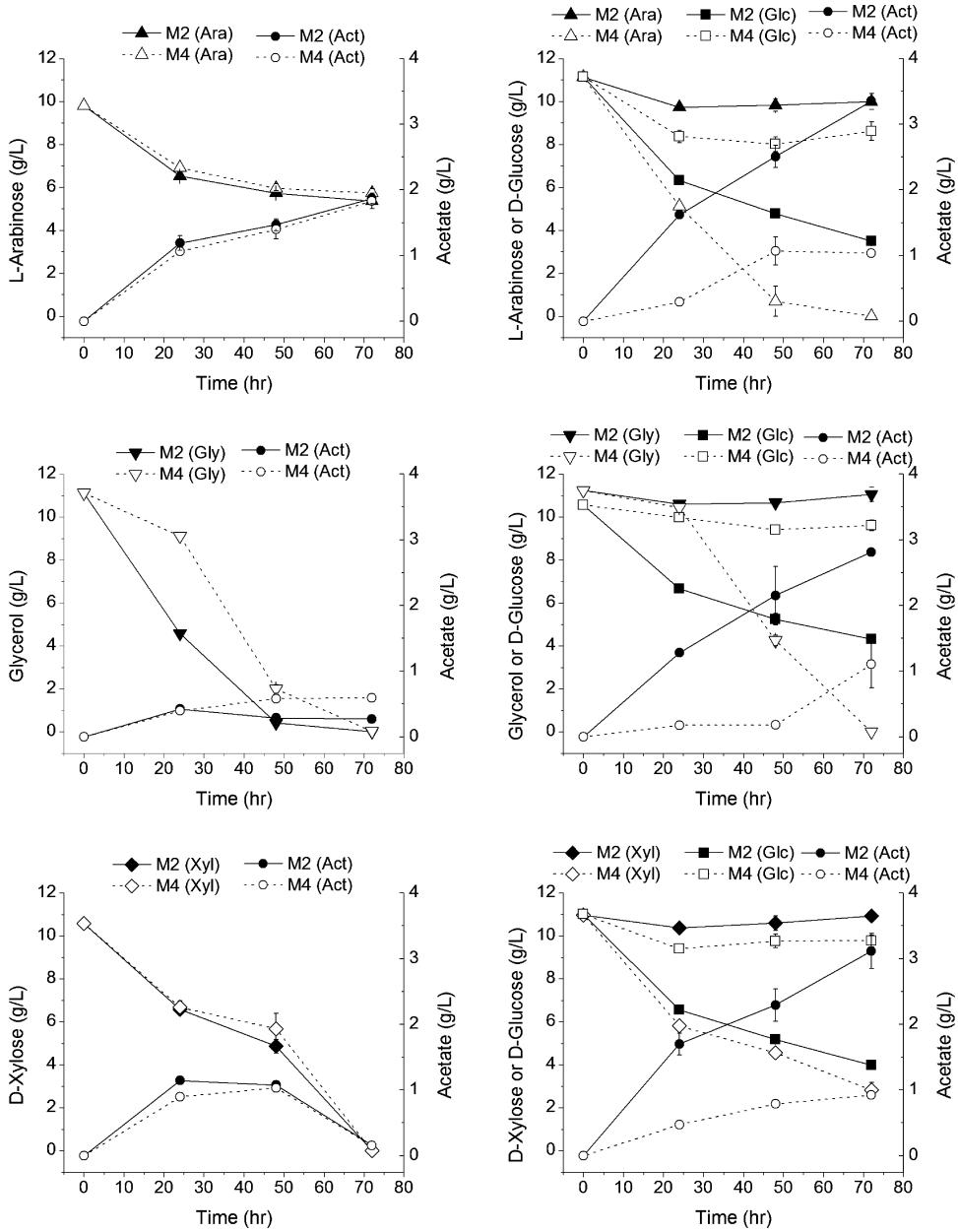

Figure 3. Carbon source and acetate ("Act," circles) concentrations in rich medium cultures of M2 (filled points, solid line) and M4 (open points, dotted lines) supplemented with L-arabinose ("Ara," triangles), glycerol ("Gly," inverted triangles), and D-xylose ("Xyl," diamonds) with D-glucose ("Glc," squares) absent (left column) or present (right column). M2: MG1655(DE3) Δ*endA* Δ*recA*; M4: MG1655(DE3) Δ*endA* Δ*recA* Δ*pgi* Δ*zwf*.

phosphatase to yield *myo*-inositol, which is oxidized to D-glucuronic acid by *myo*-inositol oxygenase (MIOX). Finally, D-glucuronic acid is oxidized to D-glucaric acid by uronate dehydrogenase (Udh). Because production of D-glucaric acid requires glucose-6-phosphate, we hypothesized that the yield of D-glucaric acid could be increased significantly in a Δ*pgi* Δ*zwf* strain.

In supplemented LB, D-glucaric acid yield on glucose is increased in the Δ*pgi* Δ*zwf* mutant nearly 18-fold over an unmutated control supplemented with L-arabinose or D-xylose, while yield is increased approximately 9-fold in the Δ*pgi* Δ*zwf* strain supplemented with glycerol (Table III). Additionally, D-glucaric acid titers are significantly higher in the Δ*pgi* Δ*zwf* mutant (Fig. 4 and Table III). We hypothesize that deletion of *pgi* and *zwf* results in higher glucose-6-phosphate pools, allowing INO1 to operate much closer to its maximum activity, which leads to increased flux through the D-glucaric acid pathway.

To simulate a lean medium that might be obtained from the hydrolysis of lignocellulosic biomass, the Δ*pgi* Δ*zwf* strain

Table III. D-glucaric acid yields on D-glucose for various carbon sources.

Strain[a]	Carbon	D-Glucaric acid titer (g/L)	Yield on D-glucose (g/g)
M2-2	L-Arabinose in LB	0.13 ± 0.01	0.044 ± 0.002
	Glycerol in LB	0.20 ± 0.02	0.052 ± 0.009
	D-Xylose in LB	0.13 ± 0.01	0.039 ± 0.002
M6	L-Arabinose in LB	0.50 ± 0.01	0.76 ± 0.13
	Glycerol in LB	0.81 ± 0.10	0.44 ± 0.04
	D-Xylose in LB	1.19 ± 0.08	0.73 ± 0.03
	L-Arabinose in MOPS	0.40 ± 0.02	0.47 ± 0.25

[a]M2-2: MG1655(DE3) Δ*endA* Δ*recA* Δ*gudD* Δ*uxaC*; M6: MG1655(DE3) Δ*endA* Δ*recA* Δ*pgi* Δ*zwf* Δ*uxaC* Δ*gudD*.

was also tested in a modified MOPS minimal medium containing 10 g/L D-glucose and 6 g/L L-arabinose. Although the strain grew more slowly under these conditions, D-glucaric acid titers of 0.40 ± 0.02 g/L were obtained, nearly as much as observed in supplemented LB (Fig. 5). The yield of D-glucaric acid from glucose was 47%; however, approximately 0.2 g/L of *myo*-inositol was also produced, bringing the total yield of G6P-derived products to 71%. *Myo*-inositol is produced from G6P as an intermediate during D-glucaric acid production and has previously been observed to build up in the culture medium under some conditions (Moon et al., 2009). Modified MOPS medium containing D-xylose and D-glucose was also tested, but no growth of the Δ*pgi* Δ*zwf* mutant was observed, possibly due to stronger residual catabolite repression of *xylAB* in minimal medium. In modified MOPS medium supplemented with D-xylose alone, M6 does not produce glucaric acid or *myo*-inositol, consistent with the expectation that glucaric acid can only be derived from glucose in a Δ*pgi* Δ*zwf* mutant (Supplementary Table SI).

Discussion

Traditionally, the main focus of metabolic engineering projects has been on increasing the final titer of a product of interest, and this approach has been widely successful for high-value compounds such as pharmaceutical intermediates and therapeutic proteins. However, increasing titers alone may not be sufficient for low-margin, high-volume bioproducts such as commodity chemicals. In these cases, product yield becomes an important process consideration, as raw material costs can be a large percentage of the manufacturing costs. Strategies that are able to increase product yield without sacrificing titer would be valuable tools for the metabolic engineer.

The use of renewable feedstocks such as lignocelluosic biomass for biochemical production presents an interesting opportunity for increasing the yield of biochemicals derived directly from glucose: in addition to glucose, lignocellulosic biomass contains several other fermentable sugars (e.g., xylose and arabinose) that may be used for biomass formation while reserving glucose solely for product

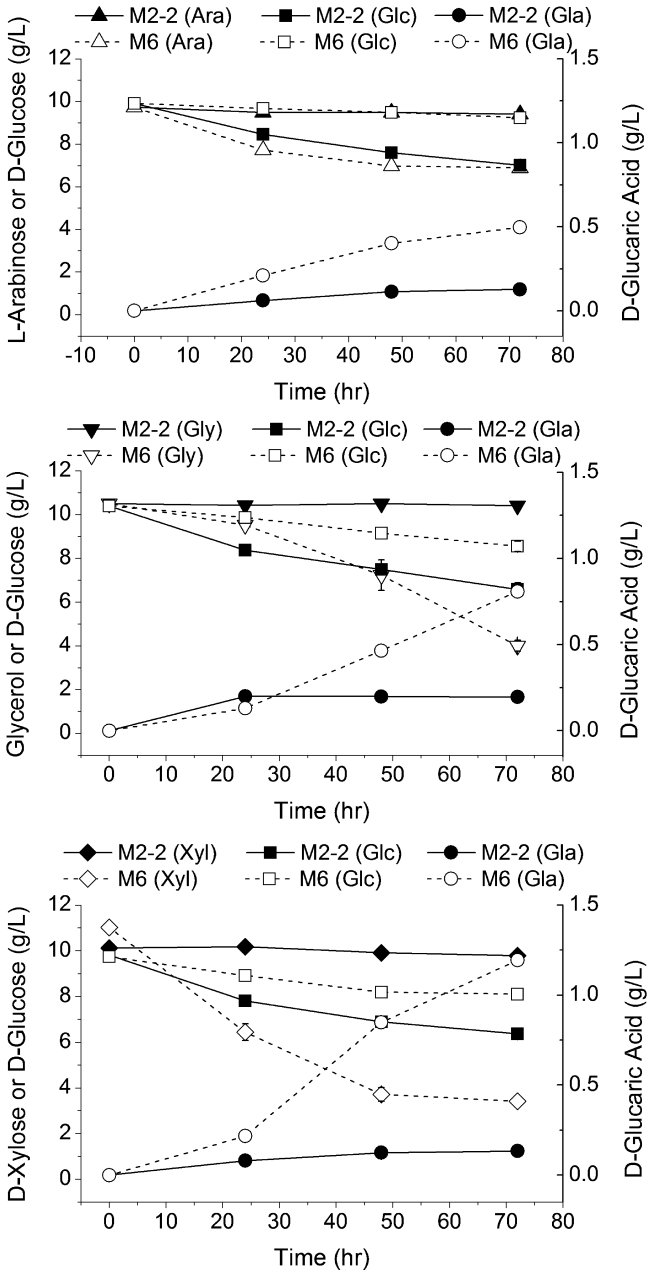

Figure 4. D-glucaric acid production ("Gla," circles) from D-glucose in strains M2-2 and M6 in rich medium. Cultures contained strain M2-2 or M6 harboring pRSFD-IN-Udh and pTrc-SUMO-MIOX and were grown in LB supplemented with D-glucose ("Glc," squares) and L-arabinose ("Ara," triangles), glycerol ("Gly," inverted triangles), or D-xylose ("Xyl," diamonds). M2-2: MG1655(DE3) Δ*endA* Δ*recA* Δ*gudD* Δ*uxaC* (filled points, solid line); M6: MG1655(DE3) Δ*endA* Δ*recA* Δ*gudD* Δ*uxaC* Δ*pgi* Δ*zwf* (open points, dotted line).

generation. Because wild-type *E. coli* preferentially consumes glucose, strain engineering is necessary to shift the cell's preference towards alternative carbon sources. In this work, we characterized the carbon source preference of a Δ*pgi* Δ*zwf* mutant and explored its ability to improve the yield of D-glucaric acid on D-glucose.

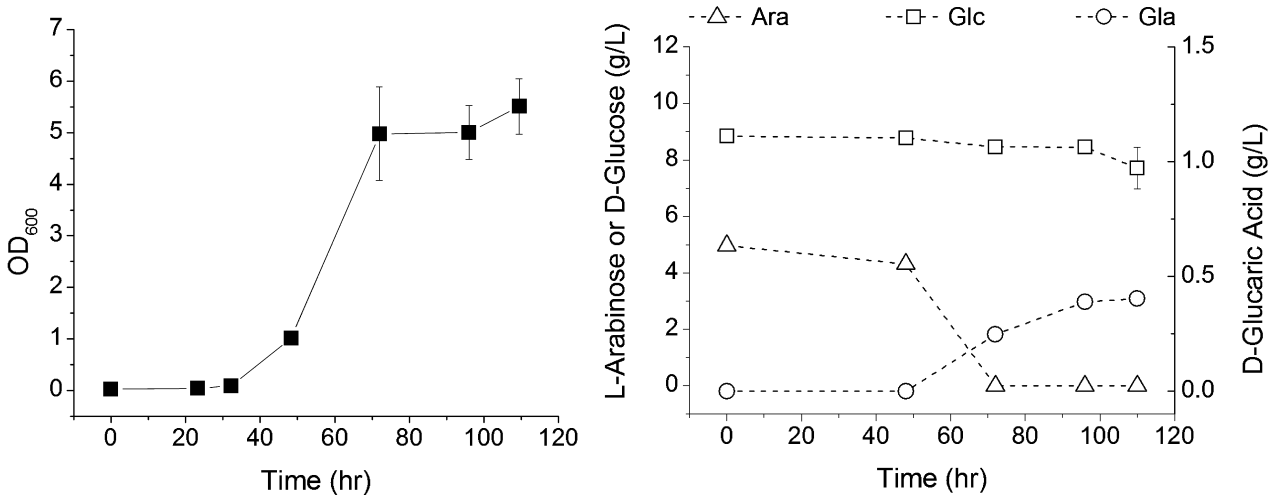

Figure 5. Growth and D-glucaric acid ("Gla," circles) production from D-glucose in strain M6 in lean medium. Cultures contained M6 harboring pRSFD-IN-Udh and pTrc-SUMO-MIOX and were grown in modified MOPS minimal medium supplemented with 6 g/L L-arabinose ("Ara," triangles) and 10 g/L D-glucose ("Glc," squares). M6: MG1655(DE3) Δ*endA* Δ*recA* Δ*gudD* Δ*uxaC* Δ*pgi* Δ*zwf*.

As expected, deletion of *pgi* and *zwf* eliminates the cell's ability to consume D-glucose for biomass formation. Catabolite repression is eliminated in this strain as well, as the Δ*pgi* Δ*zwf* mutant is able to consume L-arabinose, glycerol, and D-xylose in the presence of D-glucose. Because glucose-mediated catabolite repression occurs when glucose transport into the cell is high, we believe that intracellular buildup of glucose-6-phosphate in the Δ*pgi* Δ*zwf* mutant leads to significantly reduced glucose transport, alleviating catabolite repression. Interestingly, introduction of the D-glucaric acid pathway, which should draw down intracellular glucose-6-phosphate pools, does not appear to affect the uptake of alternative carbon sources in the presence of D-glucose. We speculate that glucose influx in the presence of INO1 is not high enough to significantly reduce the levels of phosphorylated $EIIA^{Glc}$ to result in activation of catabolite repression. Because the threshold rate of glucose import necessary for activation of catabolite repression is unknown, efforts to further increase the activity of INO1 or to introduce more active glucose consumption pathways should proceed with caution to avoid reactivation of catabolite repression.

Conclusions

In this work, we investigate the behavior of a Δ*pgi* Δ*zwf* mutant and its ability to utilize alternative carbon sources for cell growth while reserving D-glucose for product formation. This strain was able to consume L-arabinose, glycerol, and D-xylose even in the presence of D-glucose, and yields of D-glucaric acid on D-glucose were increased 9- to 18-fold in the Δ*pgi* Δ*zwf* strain. Additionally, product titers were also increased, as the initial D-glucaric acid pathway enzyme was no longer in competition with glycolytic enzymes for glucose-6-phosphate. Furthermore, the Δ*pgi* Δ*zwf* mutant exhibits similar yield increases in minimal medium, suggesting the strain's potential in an industrial setting; however, additional investigation is necessary to fully characterize the strain's robustness. These gains in product yield should easily translate to other bioproducts derived from D-glucose, and it is hoped that this strain will help improve the process economics of these value-added biochemicals.

This work was supported by the National Science Foundation through the Synthetic Biology Engineering Research Center (E.S., Grant No. EEC-0540879) and the CAREER Award program (I.M.B., Grant No. CBET-0954986), and through the Biotechnology Training Program of the National Institutes of Health (I.M.B., Grant No. T32GM008334).

References

Amann E, Brosius J. 1985. "ATG vectors" for regulated high-level expression of cloned genes in *Escherichia coli*. Gene 40:183–190.

Baba T, Ara T, Hasegawa M, Takai Y, Okumura Y, Baba M, Datsenko KA, Tomita M, Wanner BL, Mori H. 2006. Construction of *Escherichia coli* K-12 in-frame, single-gene knockout mutants: The Keio collection. Mol Syst Biol 2:2006.0008.

Balderas-Hernández VE, Hernández-Montalvo V, Bolívar F, Gosset G, Martínez A. 2011. Adaptive evolution of *Escherichia coli* inactivated in the phosphotransferase system operon improves co-utilization of xylose and glucose under anaerobic conditions. Appl Biochem Biotechnol 163: 485–496.

Chassagnole C, Noisommit-Rizzi N, Schmid JW, Mauch K, Reuss M. 2002. Dynamic modeling of the central carbon metabolism of *Escherichia coli*. Biotechnol Bioeng 79:53–73.

Curran KA, Alper H. 2012. Expanding the chemical palate of cells by combining systems biology and metabolic engineering. Metab Eng 14:289–297.

Datsenko KA, Wanner BL. 2000. One-step inactivation of chromosomal genes in *Escherichia coli* K-12 using PCR products. Proc Natl Acad Sci USA 97:6640–6645.

Gonçalves GAL, Prazeres DMF, Monteiro GA, Prather KLJ. 2013. De novo creation of MG1655-derived *E. coli* strains specifically designed for plasmid DNA production. Appl Microbiol Biotechnol 97:611–620.

Hernández-Montalvo V, Martínez A, Hernández-Chavez G, Bolivar F, Valle F, Gosset G. 2003. Expression of galP and glk in a *Escherichia coli* PTS mutant restores glucose transport and increases glycolytic flux to fermentation products. Biotechnol Bioeng 83:687–694.

Johnson DT, Taconi KA. 2009. The glycerin glut: Options for the value-added conversion of crude glycerol resulting from biodiesel production. Environ Prog 26:338–348.

Joyce BL, Stewart CN. 2012. Designing the perfect plant feedstock for biofuel production: Using the whole buffalo to diversify fuels and products. Biotechnol Adv 30:1011–1022.

Kogure T, Wakisaka N, Takaku H, Takagi M. 2007. Efficient production of 2-deoxy-scyllo-inososе from D-glucose by metabolically engineered recombinant *Escherichia coli*. J Biotechnol 129:502–509.

Lee SY. 1996. Bacterial polyhydroxyalkanoates. Biotechnol Bioeng 49:1–14.

Moon TS, Yoon SH, Lanza AM, Roy-Mayhew JD, Prather KLJ. 2009. Production of glucaric acid from a synthetic pathway in recombinant *Escherichia coli*. Appl Environ Microbiol 75:589–595.

Pandey RP, Malla S, Simkhada D, Kim BG, Sohng JK. 2013. Production of 3-o-xylosyl quercetin in *Escherichia coli*. Appl Microbiol Biotechnol 97:1889–1901.

Roe AJ, McLaggan D, Davidson I, O'Bryne C, Booth IR. 1998. Perturbation of anion balance during inhibition of growth of *Escherichia coli* by weak acids. J Bacteriol 180:767–772.

Rogers P, Chen J, Zidwick MJO. 2006. The prokaryotes. New York, NY: Springer. http://www.springerlink.com/index/10.1007/0-387-30741-9.

Sambrook J, Russell DW. 2001. Molecular cloning: A laboratory manual. Cold Spring Harbor: Cold Spring Harbor Laboratory Press.

Shiue E, Prather KLJ. 2014. Improving D-glucaric acid production from myo-inositol in *E. coli* by increasing MIOX stability and myo-inositol transport. Metab Eng 22:22–31.

Solomon KV, Moon TS, Ma B, Sanders TM, Prather KLJ. 2013. Tuning primary metabolism for heterologous pathway productivity. ACS Synth Biol 2:126–135.

Wang D, Li Q, Yang M, Zhang Y, Su Z, Xing J. 2011. Efficient production of succinic acid from corn stalk hydrolysates by a recombinant *Escherichia coli* with ptsG mutation. Process Biochem 46:365–371.

Werpy T, Petersen G. 2004. Top value added chemicals from biomass, volume 1: Results of screening for potential candidates from sugars and synthesis gas. Washington, DC: U.S. Dep. Energy. U.S. Department of Energy.

Yoon SH, Moon TS, Iranpour P, Lanza AM, Prather KLJ. 2009. Cloning and characterization of uronate dehydrogenases from two pseudomonads and *Agrobacterium tumefaciens* strain C58. J Bacteriol 191:1565–1573.

Supporting Information

Additional supporting information may be found in the online version of this article at the publisher's web-site.